Технические науки
Engineering sciences

Shear Cell Test and Hopper Design

Lukas ARNOLD[1*]
Tarun KUMAR[1**]
Joshua COWLEY[1***]
Greg WHEATLEY[1****]
Rendage Sachini Sandeepa CHANDRASIRI[2*****]

[1]James Cook University, Townsville, Australia
[2]University of Colombo, Sri Lanka

Abstract

Relevance of the work. The Hopper and Bin design is the most commonly used technique of storing materials as it is a gravity fed system and is generally used for storing materials such as agricultural grains as well as mined minerals such as sand and coal. Mass flow, which is ideally the most desired flow type sees the bulk material travel uniformly with all particles in motion until all the material leaves the bin. The other types of flow generally occur with flat-bottomed bins with shallow hoppers are not seen as ideal as with this design problems such as arching and rat holing occur. The issue with the current design is that some of the material becomes stagnant in the bin, this can be costly as if the bulk material becomes stuck, degradation can occur over time. It can be observed for the Funnel and Expanded flow, the rat holing and arching occurring due to the stagnant material.

Research Objective is to design a novel mass flow acrylic bin and hopper to store bulk quantities of sand without stagnation or degradation

Methodology. Two separate experimental procedures were carried out including the measurement of the specific gravity of the sand, shear test and final hopper design. The data was then manipulated and plotted stress transformations and identified multiple key flow property constituents. Using values such as the yield loci and associative yield stresses the hopper half angle α and opening diameter *B* were tabulated.

Results and Conclusions. The optimum opening diameter *B* for an uncompacted system is 2 mm and the hopper half angle α adjusted to 34.58°, this was tested and provided a successful mass flow hopper system. Overall, the techniques used with specific gravity and shear cell testing gave a sufficient insight into the appropriate procedure for designing efficient and accurate bin and hoppers. Then substituting the values gathered into the appropriate formulae provided a successful mass flow system for the intended bulk material which is sand.

Keywords: Hopper, Flow properties, Minerals, Bulk material properties, Geometric shape.

Introduction
Specific Gravity of Sand

Specific gravity is the ratio of the unit volume mass of soil at a stated temperature to the mass of the same volume of gas-free distilled water at a stated temperature [1]. Calculating the specific gravity of a bulk solid is an important component before the iterative shear cell testing and overall hopper design, as the degree of certainty can be found for the void ratio and degree of saturation. Void ratio is the ratio of the volume of voids (open spaces) in a soil to volume of solids. To find the specific gravity of a particular bulk solid a number of key steps including the use of a vacuum chamber, needs to be followed precisely in order to obtain correct values.

Following this, it is useful to tap or use a vibration table machine to remove more voids thus providing a more accurate result. With the respective masses of the specimen samples, the mass of the dry soil in the bottle m_s can be determined, where w is the water content of the bulk material as a decimal. The particular bulk material tested was sand and assumed that dry sand has a moisture content of 0.1% and therefore $w = 0.001$

✉Lukas.arnold@my.jcu.edu.au
**Tarun.kumar@my.jcu.edu.au
***Joshua.cowley@my.jcu.edu.au
****greg.wheatley@jcu.edu.au
(iD) https://orcid.org/0000-0001-9416-3908
*****sachini.chandrasiri7@gmail.com
(iD) https://orcid.org/0000-0003-4713-9088

in the following Equation (1) [1] which shows the mass of dry sand in the specimen bottle:

$$m_s = \frac{m_2 - m_1}{1 + w},$$ (1)

where the parameters are as following: m_1 – mass of empty bottle and stopper; m_2 – mass of bottle with sand, and stopper; w – water contents of the sand; m_s – the mass of the dry sand in the bottle.

Following this, the samples containing water can be included, for the calculation of the overall specific gravity G_s of a particular bulk material can be determined using the equation below:

$$G_s = \frac{m_s}{m_s + m_4 - m_3}.$$ (2)

Whereby the parameters are as following: m_3 – mass of bottle with sand, stopper and water (full); m_4 – mass of bottle with water (full), and stopper; G_s – the specific gravity of the sand grains.

Shear Cell Test

In order to create a mass flow system for bulk materials, several key constituents surrounding the hopper must be analysed so the optimum dimensions can be identified. These constituents are called flow properties and include values such as the angle of wall friction, angle of internal friction and wall-material cohesion [2]. The standard procedure in determining flow properties is shear testing which provides an in-depth analysis of the yield locus for the bulk material. The yield locus is used as a reference point to determine all-important constituents in creating a successful mass flow system.

The shear cell test involves a sample of the bulk material succumbing to shear force along a plane developed between the two halves of the 'shear box' after the application of a specified normal load. The shearing motion is provided by an electro-mechanically driven loading stem, which moves the bottom half of the shear box at a constant speed while measuring the reaction force on the top part of the shear box.

Hopper Design

A Perspex bin and hopper system has been requested to be designed for a mass flow bulk material of sand, this mass flow will be achieved by a successful calculation of the internal angle of wall friction. These calculations will be provided by several iterative shear cell tests including compacted and uncompacted sand, as well as shearing the Acrylic Perspex across sand particles. With these results, the yield locus and the flow functions will be determined, so all other flow properties can be identified. With the optimum angle of internal friction and opening diameter a successful mass flow system for sand will be obtained [3]. This paper will outline the procedures, calculated results and any other observed information that is relevant to the design of this storage unit. The following sections will help understand the main concepts, being the yield locus, flow function and wall friction, for calculating the two hopper parameters.

Yield Locus

The importance of the Jenike shear cell tester is that once the consolidation has occurred to the material sample several data points can be obtained and plotted to find values such as the Internal Yield Locus (IYL) and Effective Yield Locus (EYL) [4]. The Internal Yield Locus for a consolidated bulk solid is a linear line used to find the unconfined yield stress σ_c, this is ultimately the principal stress representing the strength of a material at a free surface. As the applied stress increases throughout the testing causing the point of sliding of the bulk solid sample, stress transformations or Mohr's Circle can provide limiting stress circles, which an IYL can be identified.

Using the IYL the corresponding EYL can be determined; this is a straight line from the origin to create a tangent to the larger Mohr's Circle. This is done so the initial consolidating load point can be determined, the angle from the horizontal origin is important as it is the effective angle of internal friction [5]. With the consolidating load point determined the Major Consolidating Principal Stress σ_{mc} can be determined, this is the major principal stress due to the initial consolidating load. It is determined by drawing a Mohr's Circle through the consolidating load point and tangent to the IYL. The formulae used to draw the Mohr's circle such as distance and radius are as follows:

$$d = \frac{c_w}{\tan(\varphi)};$$ (3)

$$r = \frac{d \sin \varphi}{1 - \sin \varphi},$$ (4)

where d – Distance from origin (x-axis); c_w – Wall cohesion; φ – Wall friction angle; r – Radius of the Mohr's circle.

Flow Function

The ability for a material to flow and its overall strength can be determined by creating a flow function. The flow function is the relationship between the unconfined yield stress σ_c and the major consolidating principal stress σ_{mc}. There are multiple factors that must be considered when trying to determine the flow function of a bulk material, these can include the moisture content, storage time and vibration [6]. To incorporate these factors the flow function calculations, require shear testing several different samples each with a different consolidating load. A flow function can be plotted by using several yield loci, the yield loci from each test determines the intercept points on the plot [7]. A material's cohesiveness generally illustrates the slope of the flow function on the plot, where the less cohesive a bulk material is, the easier it will flow, in which design requirements must be adjusted to cater this.

The formulae to find the unconfined yield stress σ_c, the major consolidating principal stress σ_{mc} and the angle of internal friction δ are as follows:

$$\sigma_c = 2r;$$ (5)

$$\sigma_{mc} = \sigma_m + \frac{\tau_w \sin \varphi}{\cos \varphi} + \frac{\tau_w}{\cos \varphi};$$ (6)

$$\delta = \tan^{-1}\left(\frac{\tau_w}{\sigma_{mc}}\right),$$ (7)

where τ_w – Wall shear stress.

Wall Friction

When calculating the flow properties and composition for a bulk so lid it is important to consider the affect the material has on the apparent wall material for the hopper and bin. Shear testing a bulk solid material against the material of what the bin and hopper will be constructed is important as it can identify flow constituents such as the walls yield locus and the angle of wall friction [8]. The process is the same as testing just the bulk material but with more information regarding the design material, the higher the chances of creating a mass flow system. Below is the formula used along with the shear cell tested results to find the wall shear stress:

$$\mu_w = \mu\sigma_w + c_w, \tag{8}$$

where μ_w – Coefficient of wall friction; σ_w – Wall normal stress.

With the shear stress determined between the wall and the bulk solid, the values can be plotted with a Mohr's circle and the angle of wall friction φ_w can be made as a correlation to the slope of the wall yield locus. Fig. 1 below is an example plot of wall shear stress against wall normal stress, this plot outlines the yield locus between the bulk solid and the wall material as well as the location of the angle of wall friction [1].

$$\varphi_w = \tan^{-1}(\mu_w)(\mu_w). \tag{9}$$

It is also important to consider how the bin and hopper will operate throughout its life, if bulk materials spends a continuous amount of time in the bin it must be accounted [9]. Some materials gain adhesive stress when kept at rest for long periods of time, so time tests are used to measure the static friction and overall strength between the two materials when kept at rest [3].

Finally, the hopper half angle α and the opening diameter β can be determined; these can be considered the most important parameters regarding hopper design. Fundamentally these values are the main stakeholder in calculating an accurate mass flow system, there are many other constituting values that will be used to find these principles and their relevant formulae are as follows:

$$\Omega = \sin^{-1}\left[\frac{\sin \varphi\, avg}{\sin \delta\, avg}\right]; \tag{10}$$

$$\beta = \frac{\varphi\, avg + \Omega}{2}; \tag{11}$$

$$\alpha = 90 - (0{,}5)\cos^{-1}\left(\frac{1 - \sin \delta\, avg}{2\sin \delta\, avg}\right) - \beta; \tag{12}$$

$$\bar{\sigma} = \frac{\sigma_{mc\, critical}}{ff}; \tag{13}$$

$$\rho\, sand = SG\, sand \cdot \rho\, H_2O \text{ at } 25\,^{\circ}C; \tag{14}$$
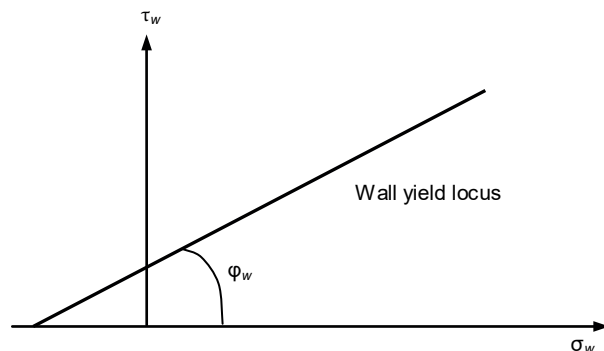
$$B = \frac{\sigma_1 H(\alpha)}{g\rho\, sand}. \tag{15}$$

Figure 1. Wall Shear Stress against Wall Normal Stress.
Рисунок 1. Напряжение сдвига на стенке относительно нормального напряжения стенки.

Methodology

To complete the experimental side of this practical, two separate experimental procedures were carried out which includes measurement of the specific gravity of the sand, the shear test and the final hopper design. To measure the specific gravity of sand, weight of two 250 ml bottles was measured and labelled separately as 4 and C. The bottles were then filled up with water until no water flow occurred when the stopper was inserted and the weight and temperature was measured. Then the water was removed and fine sand (bulk solid material) was filled to the dried bottles up to 150 ml and the weight was measured. Water was added up to 200 ml and placed on a vacuum pump for 10 minutes to remove entrapped air. After all entrapped air was removed the bottle was filled with water until no excess water was present. The mass and temperature of each bottle was weighed.

The shear cell test was conducted by well cleaning the shear box and halves. Then the two halves of the shear box were screwed together with a friction screw loose and screwed down until they touch. The base plate was placed in by assuring the groves were parallel with the shear direction. Porous stones were placed with rough surface facing the material. The shear box was then slowly filled with sand, assuring the sand was not compacted. The sand height was controlled by the depth gauge making a perfectly flat top. The second porous stone was placed on top by facing the rough side to the material and then the shear box was weighed. After that the top plate was placed on top with the groves parallel to shear direction and placed on a shearmatic. The horizontal locking screws were tightened and 10 kN vertical load was locked in place. Then the vertical displacement transducer was placed on the vertical platform and horizontal displacement transducer was set to its medium any measurements were taken.

To design the hopper adjustable acrylic hopper was adjusted to have the angle and opening dimensions of the optimum for mass flow [10]. The gap was closed with another piece of acrylic and sand was poured into the top and the gap was opened allowing the sand to flow. The flow type was observed. Then the angle and opening width was tested for different values to test if a variance of dimensions causes funnel flow.

Results and Calculations

All experimental and calculated results are shown in the following tables with sample calculations given for the first two experimental procedures.

Specific Gravity Experiment

To calculate the specific gravity of the sand, the specific gravity experimental methodology was carried out to yield the following data given in Table 1.

Table 1. Specific gravity experiment results.
Таблица 1. Результаты эксперимента по удельному весу.

Parameter	Tests	
	Test Glass (C)	Test Glass (4)
Water temperature, °C	26	27
m_1, g	138.341	141.474
m_2, g	360.888	340.366
m_3, g	571.668	507.254
m_4, g	438.283	388.539
w, %/100	0.001	0.001
m_s, g	222.325	198.693
G_s, g	2.499	2.484

Note: m_1 – mass of empty bottle and stopper; m_2 – mass of bottle with sand, and stopper; m_3 – mass of bottle with sand, stopper and water (full); m_4 – mass of bottle with water (full), and stopper; w – water contents of the sand; m_s – the mass of the dry sand in the bottle; G_s – the specific gravity of the sand grains.

These values were then used in Equations (1)–(2) to yield the specific gravity of sand. For test glass C, the following calculations were computed:

$$m_s = \frac{m_2 - m_1}{1 + w};$$
(1)

$$m_s = \frac{360.888 - 138.341}{1 + 0.001};$$

$$m_s = 222.325 \text{ g};$$

$$G_s = \frac{m_s}{m_s + m_4 - m_3};$$
(2)

$$G_s = \frac{222.325}{222.325 + 438.283 - 571.668};$$

$$G_s = 2.499.$$

The two specific gravity results are then averaged as shown below:

$$G_{s,\,avg} = \frac{G_{s,1} + G_{s,2}}{n};$$

$$G_{s,\,avg} = \frac{2.499 + 2.484}{2};$$

$$G_{s,\,avg} = 2.492.$$

Shear Cell Test Experiment

The purpose of shear cell test is to design hoppers, and hopper design has two major parameters, one is hopper half angle α, another is the minimum hopper opening *B* [11]. The shear cell test is important to determine these two major parameters. it gives results that can develop an IYL and an EYL, based on this, the unconfined yield strength σ_c can be determined by drawing a Mohr's circle that related to IYC and origin, the major principal stress σ_{mc} can be determined by drawing a Mohr's circle that related to IYC and consolidation point, which in this practical is the point that gives 100 kPa vertical pressure plus the pressure from the top cap of the shear cell box. Furthermore, the effective angle of internal friction δ and angle of internal friction φ can be determined from EYL and IYL respectively, these two parameters can give the hopper half angle α by using half angle equation for slot hopper in this practical, with the parameter of α and δ the flow factor *ff* then can be determined by using an appropriate figure, then the *H* (α) can be determined using the figure with α and *ff* parameters.

This *ff* can also be expressed in form of $\overline{\sigma}_c / \sigma_{mc}$, where $\overline{\sigma}_c$ is stable arch stress, the flow function *FF* can be expressed in form of σ_c/σ_{mc}, the critical principle arch stress is at where an intersection point of *ff* line and FF line $\overline{\sigma}_c = \sigma_c$, once find out the critical point, once get the *H* (α) and $\overline{\sigma}_c$ the minimum hopper opening *B* can be determined. The hopper design results and al l the relevant parameters are determined from the shear cell test data, which the shear cell test is necessary and is the major purpose of the hopper design.

The shear cell test was carried out using the shear cell apparatus and methodology. The weights of all the shear cell boxes, with sand and porous stone/acrylic are shown in Table 2 below.

Table 2. The weights for shear boxes and sand for all tests.
Таблица 2. Вес сдвиговых коробок и песка для всех испытаний.

Test Type	Mass w/o Top Cap, g
Sand uncompacted – 25	3922.5
Sand uncompacted – 50	3849.9
Sand uncompacted – 100	3843.7
Sand compacted – 25	3841.8
Sand compacted – 50	3852.2
Sand compacted – 100	3847.4
Acrylic uncompacted – 25	3690.0
Acrylic uncompacted – 50	3730.0
Acrylic uncompacted – 100	3732.6
Acrylic compacted – 25	3745.1
Acrylic compacted – 50	3734.2
Acrylic compacted – 100	3738.6

The apparatus items without sand were also measured and are shown in Table 3 below.

Table 3. The weights of the apparatus items used for shear testing.
Таблица 3. Вес предметов оборудования, используемых для испытания на сдвиг.

Apparatus Item/s	Weight, g
Box + 2 Stone	3491.2
Box + 15 mm Acrylic + 1 Stone	3532.8
Mass Top Cap	1192.1

To determine the additional pressure P that the top cap adds to the vertical load, the mass of the top cap is used and converted to pressure as shown in the following sample calculation. The dimensions of the top cap are 100 mm by 100 mm.

$$F_w = mg; \qquad (16)$$

$$F_w = (1.1921)(9.81);$$

$$F_w = 11.6945 \ N;$$

$$P = \frac{F}{A}; \qquad (17)$$

$$P = \frac{11.6945}{10000};$$

P = 0.00116945 MPa or 1.16945 kPa.
These calculated values are summarised in Table 4.

Table 4. The summarised values for the top pressure calculation.
Таблица 4. Обобщенные значения для расчета верхнего давления.

Parameter	Value
Mass Top Cap, kg	1.192
Force Weight, N	11.695
Area, mm²	10 000
Pressure, MPa	0.001169
Pressure, kPa	1.16945

From the experimental tests, data was collected and used for analysis purposes by inserting to an excel sheet, in there the normal stress is the vertical adjusted pressure and remains relatively constant due to that being the consolidating stress input into the machine. The Shear stress was calculated by dividing the horizontal force by the area of shear, being the 100 mm by 100 mm [12]. This was computed for each of the 12 tests and the maximum shear stress value was determined using the Excel max function as shown below:

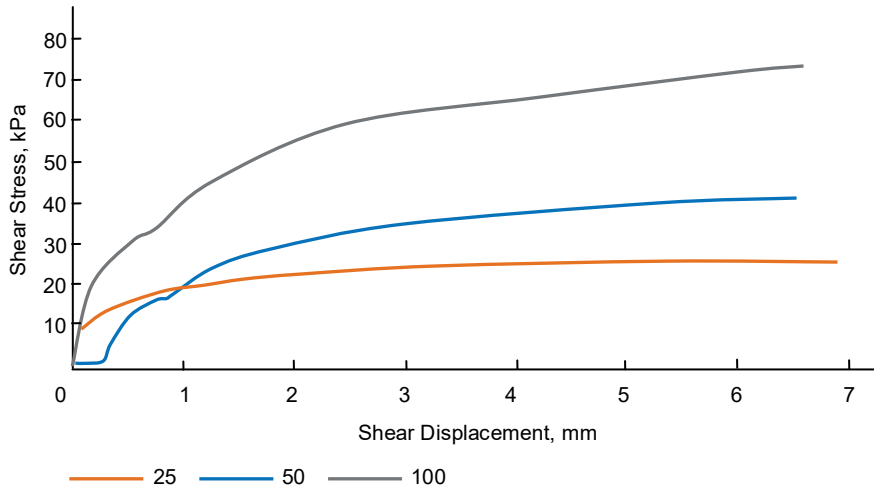Maximum shear stress value = MAX (AJ2 : AJ798).

The normal stress value is the corresponding normal stress value to that of the maximum shear stress. This was found using the lookup function as shown below:

Corresponding normal stress = LOOKUP (AJ799, AJ2 : AJ798, Al2 : Al798).

This was computed for each of the 12 tests and summarised versions of the values are displayed in Table 5.

To graphically display the maximum shear stresses, and to visually prove the shear stress values in Table 5 are correct, the shear stress was graphed against the shear displacement to give the following Fig. 2 to 5. The shear cell test in this practical was a strain-controlled test, which the shear force was applied in equal increments until the specimen fails, and only the peak shear strength was observed for further calculation. Fig. 2 to 5 below present the maximum shear stress is at the point where the specimen just begins to fail.

Shear test result Fig. 2 and 3 with porous stone top plate presented that the shear stresses increased gradually until they had reached a constant value which is called ultimate shear stress (or residual shear stress), for the shear test with acrylic top plate in the Fig. 5, the shear stresses increased dramatically over a short shear displacement, then slowly increased over a long shear displacement, finally they had reached the ultimate shear stress. For each type of the top plate been used for the test, the compacted tests had similar trend as uncompacted tests, and they do not have a significant peak shear strength, this can be the reason that the sand was not dense enough in compacted tests, and the vertical normal load was not great enough, these resulting the sand was still loose sand or normally consolidated sand, the theoretical plot for the shear stress against horizontal shear displacement is shown in Fig. 6 above.

Table 5. The maximum values from each of the tests.
Таблица 5. Максимальные значения по каждому из тестов.

Test Type	Maximum Stresses, kPa	Test 1 (25)	Test 2 (50)	Test 3 (100)
Uncompacted Sand	Normal	26.659	51.692	101.670
	Shear	26.428	41.236	73.756
Compacted Sand	Normal	101.670	51.649	102.237
	Shear	73.756	41.344	82.038
Acrylic Uncompacted	Normal	26.681	51.627	101.649
	Shear	15.458	24.434	36.098
Acrylic Compacted	Normal	26.681	51.671	101.649
	Shear	16.369	25.799	46.309

Figure 2. Shear Stress against Shear Displacement for Uncompacted Sand.
**Рисунок 2. Напряжение сдвига по сдвиговому смещению для неуплотненного песка.**
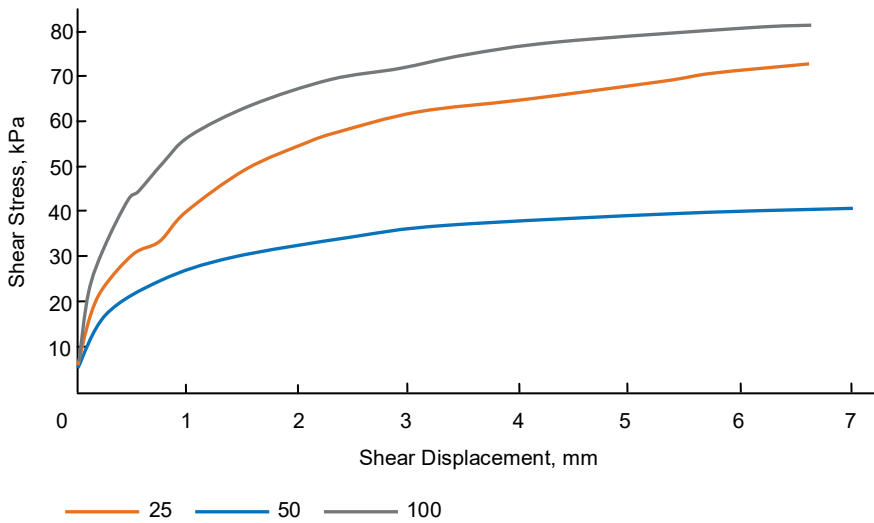
Figure 3. Shear Stress against Shear Displacement for Compacted Sand.
Рисунок 3. Напряжение сдвига по сдвиговому смещению для уплотненного песка.
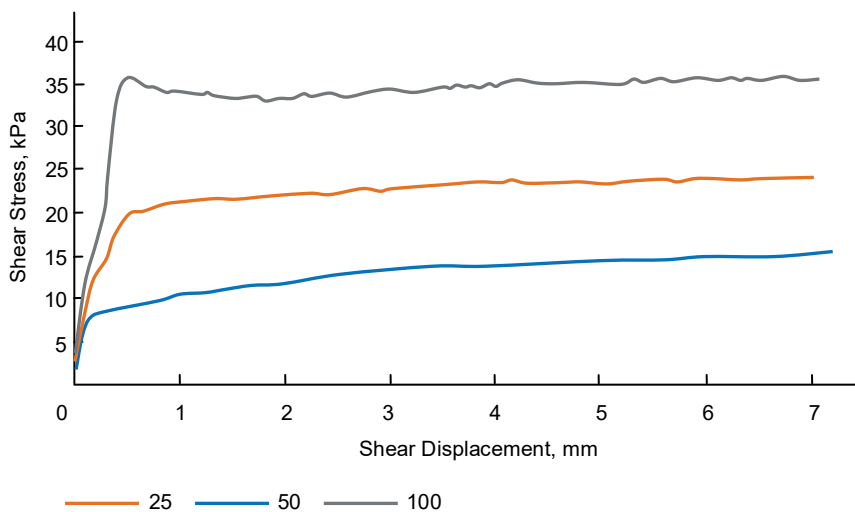
Figure 4. Shear Stress against Shear Displacement for Acrylic Uncompacted.
Рисунок 4. Напряжение сдвига по сдвиговому смещению для неуплотненного акрила.
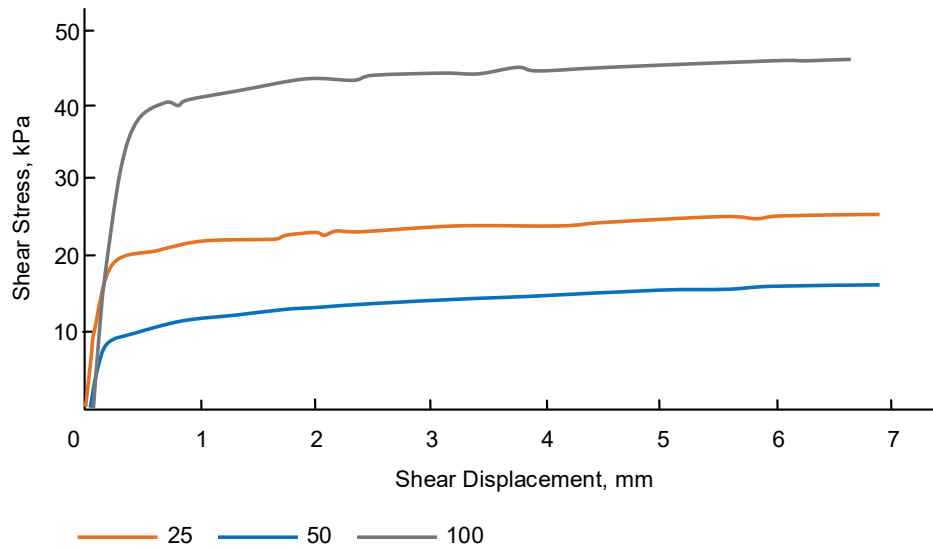
Figure 5. Shear Stress against Shear Displacement for Acrylic Compacted.
Рисунок 5. Напряжение сдвига по сдвиговому смещению для уплотненного акрила.
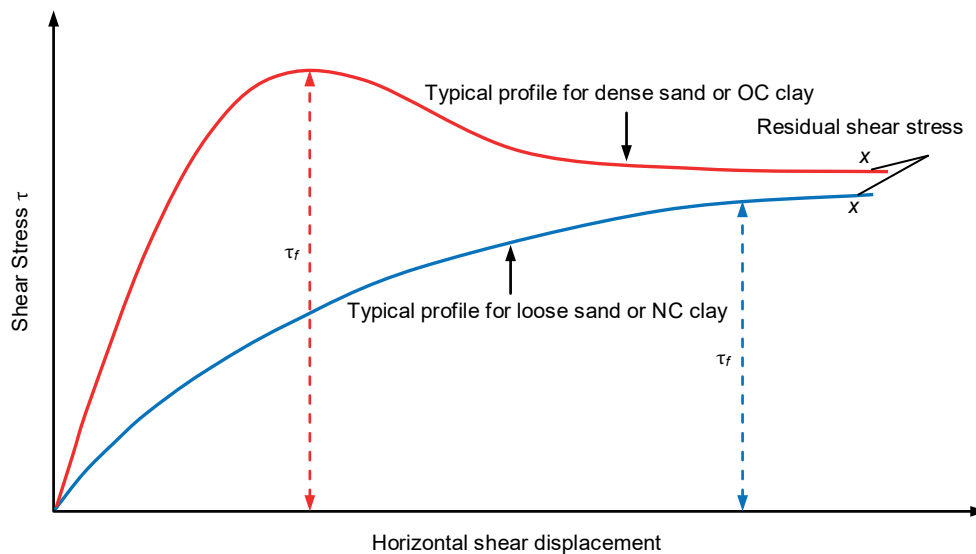
Figure 6. Typical shear stress versus horizontal shear displacement (OC stands for over consolidated and NC stands for normally consolidated) [5].
Рисунок 6. Типичное напряжение сдвига в зависимости от горизонтального сдвига (OC означает «чрезмерно консолидированный», а NC означает «нормально консолидированный») [5].

The similarity of all the tests was the higher vertical load gives higher shear stress, the differences was that under the same vertical load, the compacted tests had higher shear force over the shear displacement compared to the uncompacted tests, the maximum rate of increase shear stress is 28.29% for the acrylic top plate under 100 kPa vertical load, it is shown in Table 6. The table also showed that under the same sand condition (compacted or uncompacted), the tests with porous stone had significant increase rate compare to the acrylic plate, the maximum rate is 104.32% for the uncompacted condition with both 100 kPa vertical load.

Hopper Design Experiment

To determine the two hopper design parameters being the hopper half angle α and the minimum slot opening *B* the following hopper design calculations were carried out. From the shear cell test experiment the maximum shear stress and corresponding normal stress were defined. These values are now used to find the two design parameters.

The data from Table 6 was used to generate the following graphs of the shear stress against the normal stress. Linear trend lines were added with supporting equations and *r*-squared value.

From above Fig. 7 to 10, it can be seen that a linear trend line follows the data points collected from the shear cell test for the tests with accurate data. It can again be seen that the data for the compacted test is incorrect and be excluded from further calculations. For the graphs with accurate data, the *r*-squared value is very close to one and therefore the data is considered fairly accurate.

Table 6. Maximum shear stress comparison.
Таблица 6. Сравнение максимального напряжения сдвига.

Load, kPa	Maximum shear stress, kPa			Maximum shear stress, kPa		
	Uncompacted porous stone plate	Compacted porous stone plate	Increase in shear stress, %	Uncompacted acrylic plate	Compacted porous stone plate	Increase in shear stress, %
25	26.428	N/a	N/a	15.458	26.428	70.970
50	41.235	41.344	0.260	24.433	41.236	68.770
100	73.756	82.038	11.230	36.098	73.756	104.320
Load, kPa	Uncompacted acrylic plate	Compacted acrylic plate	Increase in shear stress, %	Compacted acrylic plate	Compacted porous stone plate	Increase in shear stress, %
25	15.458	16.369	5.890	16.369	N/a	N/a
50	24.433	25.799	5.590	25.799	41.344	60.250
100	36.098	46.309	28.23	46.309	82.038	77.150

$y = 0.6338\,x + 9.1098$

$R^2 = 0.9995$
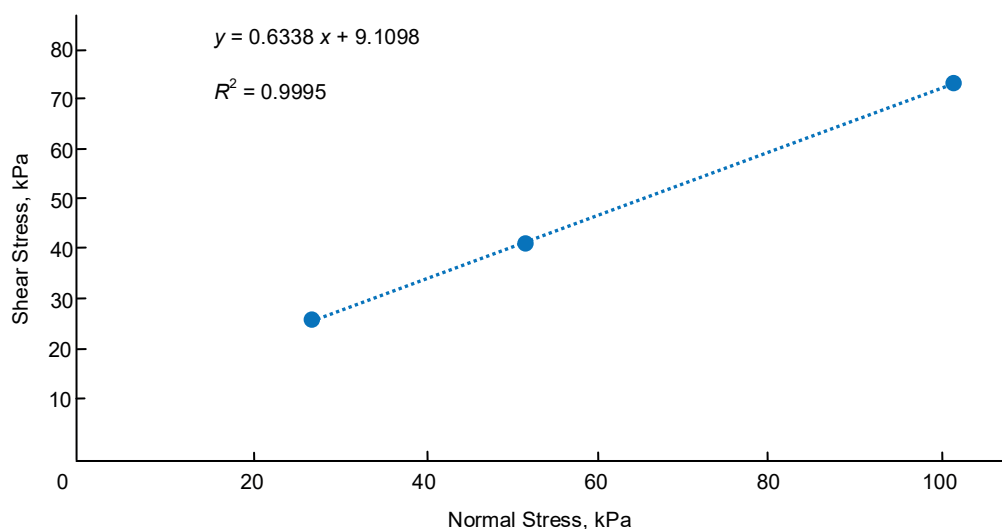
Figure 7. Shear Stress against Normal Stress for Uncompacted Sand.
Рисунок 7. Напряжение сдвига по нормальному напряжению для неуплотненного песка.

$y = 0.2107\,x + 53.071$

$R^2 = 0.14$
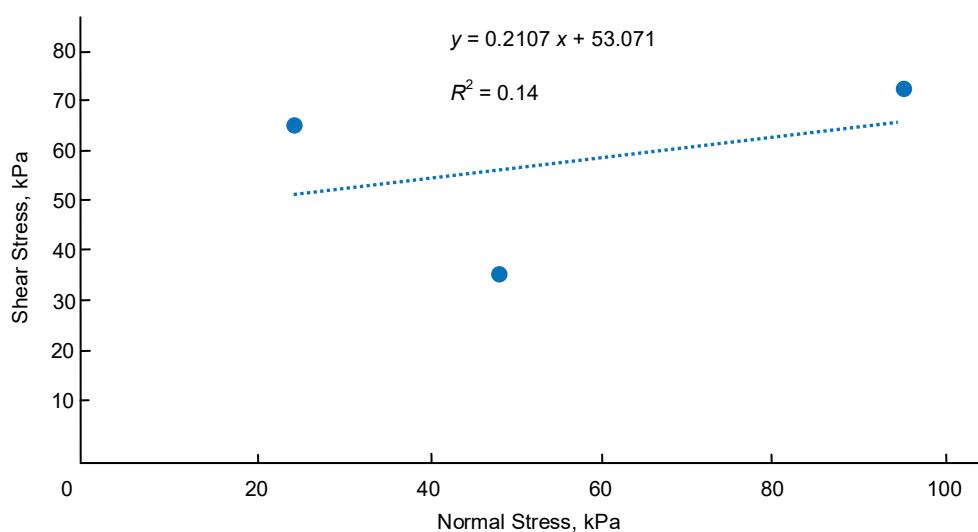
Figure 8. Shear Stress against Normal Stress for Compacted Sand.
Рисунок 8. Напряжение сдвига по нормальному напряжению для уплотненного песка.
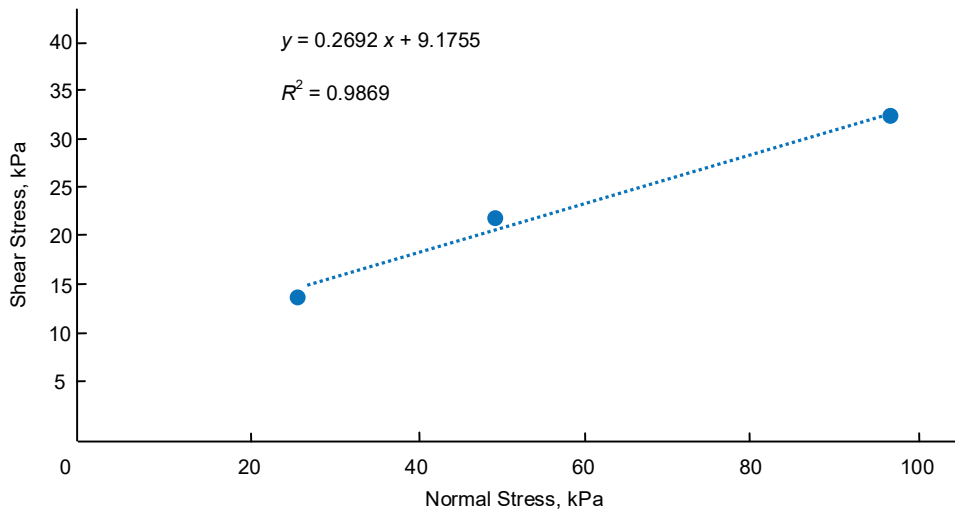
$y = 0.2692\,x + 9.1755$

$R^2 = 0.9869$

Figure 9. Shear Stress against Normal Stress for Acrylic Uncompacted.
Рисунок 9. Напряжение сдвига по сравнению с нормальным напряжением для неуплотненного акрила.

$y = 0.4007\,x + 5.4447$
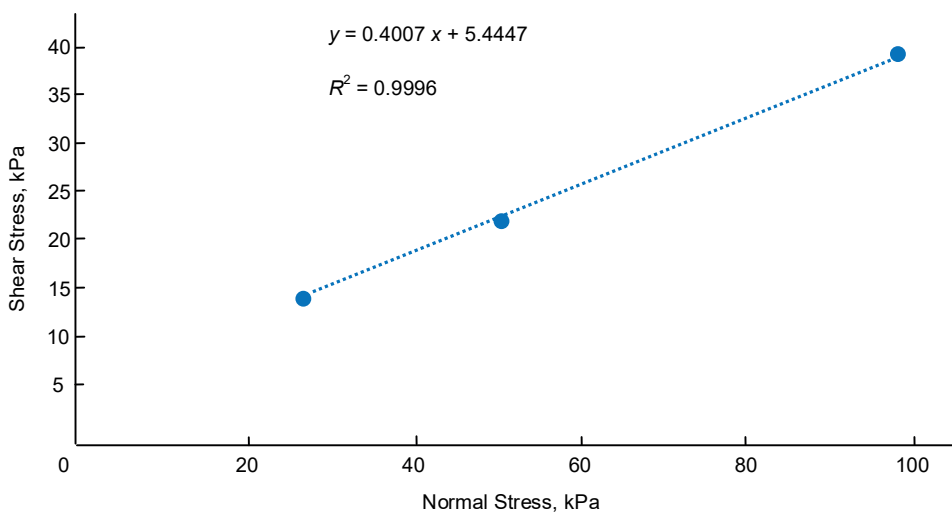
$R^2 = 0.9996$

Figure 10. Shear Stress against Normal Stress for Acrylic Uncompacted.
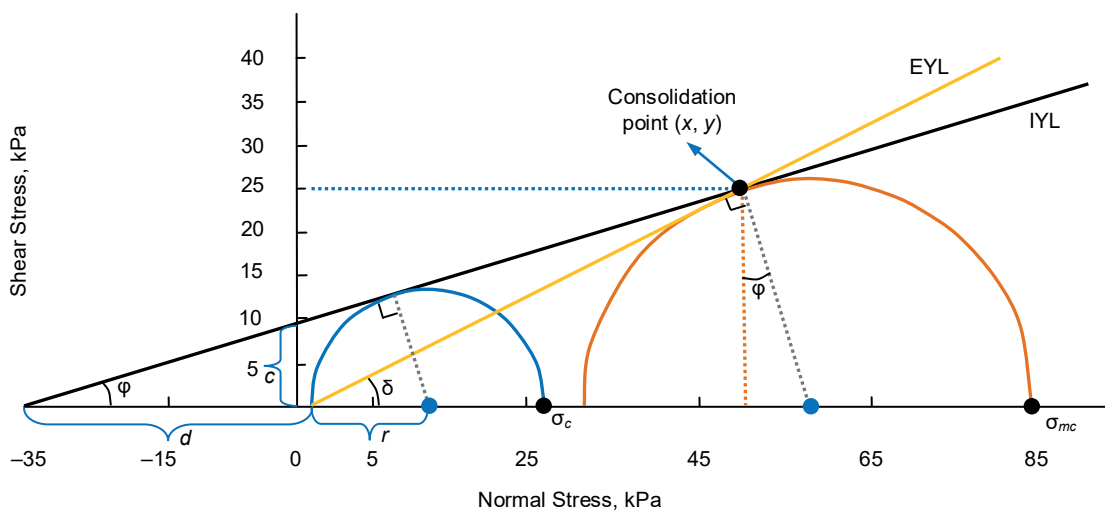**Рисунок 10. Напряжение сдвига по сравнению с нормальным напряжением для уплотненного акрила.**

Figure 11. Sketch of Mohr's circle and yield locus.
Рисунок 11. Схематическое изображение круга Мора и кривой текучести.

Since Figures have given the linear trend line and this line can be used as IYL, therefore the terms of φ, δ, σ_c and σ_{mc} can be determined and calculated using trigonometric, and these terms are presented in Figure below. The gradient angle of IYL line is φ, and the gradient angle of EYL lines is δ, the intersection point of y-axis and IYL is the cohesive value of the test specimen. The first Mohr's semi-circle is that started from the origin and tangent to the IYL, this can determine the σ_c which is at the intersection point of first Mohr's circle and the x-axis [13]. The second Mohr's semi-circle is that passing the consolidation point and tangent to the IYL, the point σ_{mc} is at the intersection point of second Mohr's circle and the x-axis [14].

The trend line equations were then used to determine the cohesion and the friction angle since the equations match equation (8) shown below. The friction coefficient was also converted to frictional angle using equation (9) as shown in the following. These values were summarised into Table 7;

$$\tau_w = \mu\sigma_w + c_w; \tag{8}$$

$$\varphi = \tan^{-1}(\mu); \tag{9}$$

$$\varphi = \tan^{-1}(0.6338);$$

$$\varphi = 32.3665°.$$

To determine the unconfined yield stress and the major consolidating stress for further calculation the calculations to define the family of yield loci were computed. To calculate the distanced before the origin on the x-axis for the IYL equation (3) was used as shown below:

$$d = \frac{c_w}{\tan(\varphi)}; \tag{3}$$

$$d = \frac{9.109}{\tan(32.366)};$$

$$d = 14.3733 \text{ kPa.}$$

To find the radius of the unconfined Mohr's circle, equation (4) was used as shown below:

$$r = \frac{d \sin \varphi}{1 - \sin \varphi}; \tag{4}$$

$$r = \frac{14.373 \sin(32.366)}{1 - \sin(32.366)};$$

$$r = 16.559 \text{ kPa.}$$

The unconfined yield stress can now be calculated using equation (5):

$$\sigma_c = 2r; \tag{5}$$

$$\sigma_c = 2\,(16.559);$$

$$\sigma_c = 33.118 \text{ kPa.}$$

The major points from figures were also noted and equations (6) and (7) were used to calculate the major consolidation stress and the angle δ. Using the major points $\sigma_m = 101.6705$ and $\tau_w \text{TW} = 73.7561$ the following is calculated:

$$\sigma_{mc} = \sigma_m + \frac{\tau_w \sin \varphi}{\cos \varphi} + \frac{\tau_w}{\cos \varphi}; \tag{6}$$

$$\sigma_{mc} = \sigma_m + \frac{(73.756)\sin(32.366)}{\cos(32.366)} + \frac{73.756}{\cos(32.366)};$$

$$\sigma_{mc} = 235.958 \text{ kPa;}$$

$$\delta = \tan^{-1}\left(\frac{\tau_w}{\sigma_{mc}}\right), \tag{7}$$

$$\delta = \tan^{-1}\left(\frac{73.756}{101.671}\right),$$

$$\delta = 35.959°.$$

From this all relevant data is summarised in Table 8 below and from this Family of Loci graphs are created and shown in Fig. 12–14.

The values of φ, δ, σ_c and σ_{mc} for each type of test are presented in Table 8: Terminology and Values. According to Table 8 the maximum σ_{mc} was 234.0691 kPa for the uncompacted sand.
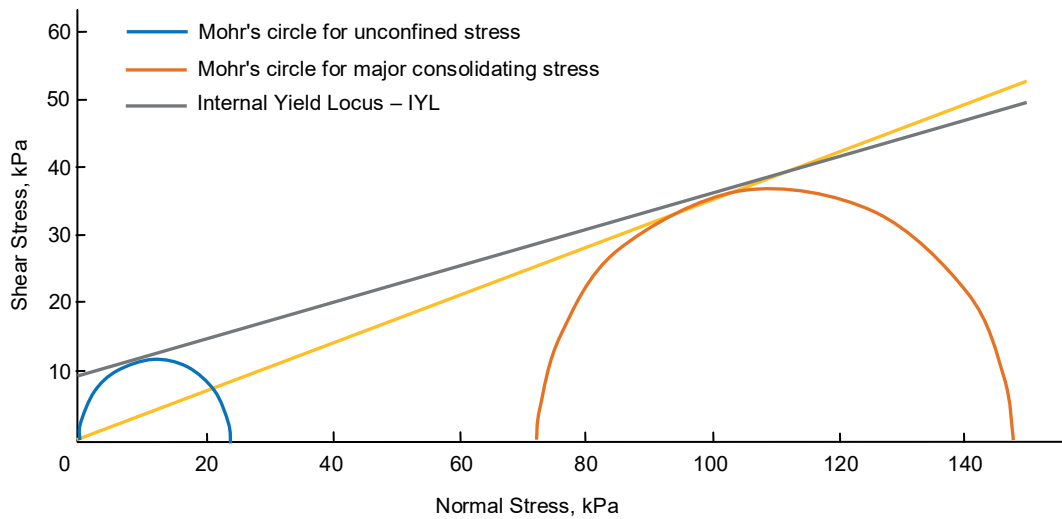
Table 7. Terminology and Values.
Таблица 7. Терминология и значения.

Parameter	Uncompacted sand	Acrylic Uncompacted	Acrylic Compacted
Wall Cohesion c_w	9.109	9.175	5.445
Coefficient of wall friction μ	0.634	0.269	0.401
Wall friction angle φ, degrees	32.367	15.067	21.836
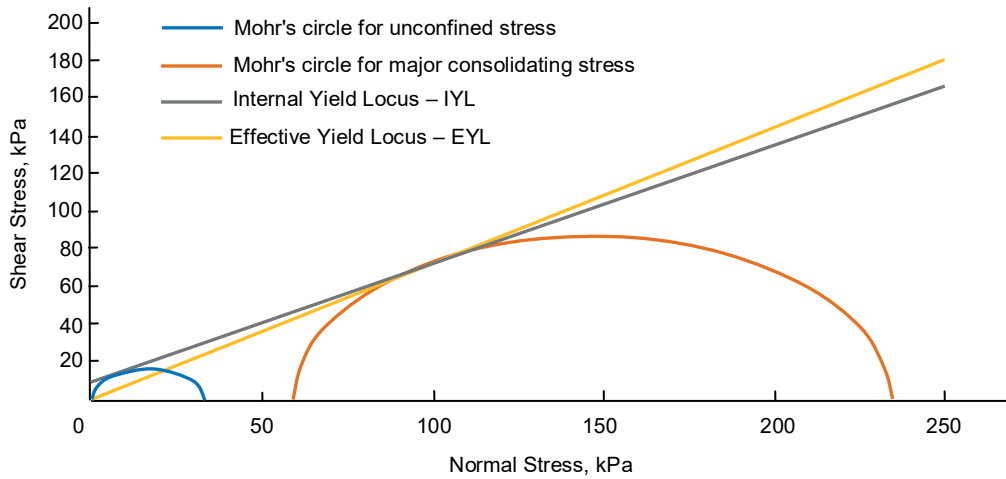
Figure 12. Family of Yield Loci for Uncompacted Sand.
Рисунок 12. Группа кривых текучести неуплотненного песка.

Figure 13. Family of Yield Loci for Acrylic Uncompacted.
Рисунок 13. Группа кривых текучести для акриловых неуплотненных материалов.
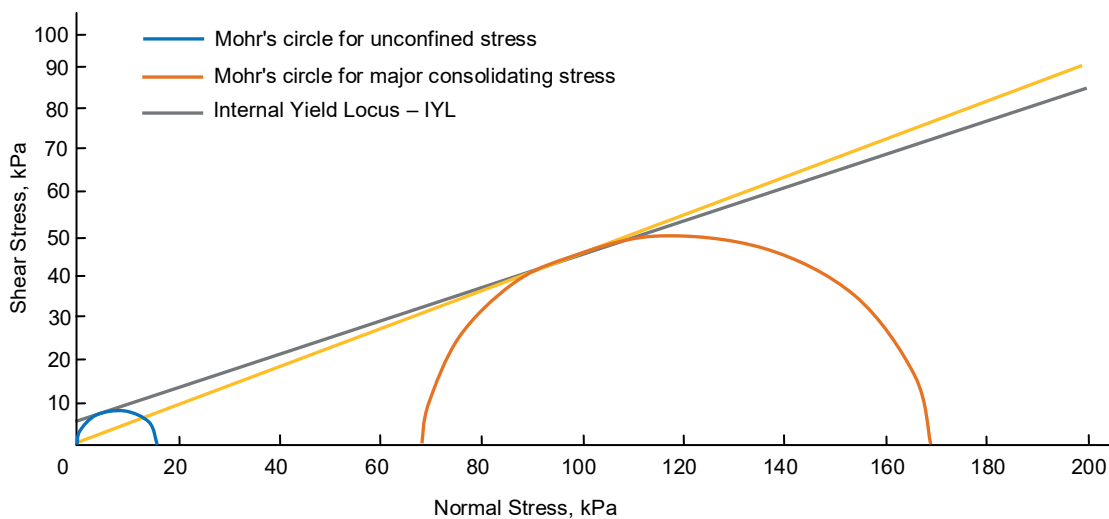
Figure 14. Family of Yield Loci for Acrylic compacted.
Рисунок 14. Группа кривых текучести для уплотненного акрила.

Table 8. Terminology and Values.
Таблица 8. Терминология и значения.

Parameter	Uncompacted Sand	Compacted Sand	Acrylic Uncompacted	Acrylic Compacted	Average for uncompacted
c, kPa	9.109	53.071	9.175	5.445	31.090
φ, degrees	32.366	11.899	15.067	21.836	16.870
d, kPa	14.373	251.879	34.084	13.588	–
r, kPa	16.559	65.418	11.972	8.047	–
σ_c, kPa	33.118	130.837	23.944	16.094	28.530
x (major point), kPa	100	100	100	100	100
y (major point), kPa	73.756	82.038	36.097	46.309	60.030
σ_{mc}, kPa	234.069	201.125	147.100	168.444	190.580
δ, degrees	36.411	39.365	19.848	24.848	28.130

Table 9. Values for compacted and uncompacted.
Таблица 9. Значения для уплотненных и неуплотненных материалов.

Parameter	Uncompacted	Compacted
σ_c, kPa	28.534	16.090
σ_{mc}, kPa	192.244	170.090
c, kPa	9.193	5.445
φ, degrees	23.716	21.835
δ, degrees	27.755	24.493

There are two major parameters to design a hopper, hopper half angle a and hopper opening *B*. In order to get these two values some basic parameters need to be determined from the shear cell test, which are unconfined stress s_c, major consolidation stress s_{mc} internal friction angle φ, effective internal friction angle d, and stable arch stress $\bar{\sigma}_c$. Using equations (10) to (12) the appropriate values can be found below:

Hopper Half Angle:

$$\Omega = \sin^{-1}\left[\frac{\sin \varphi\, avg}{\sin \delta\, avg}\right]; \qquad (10)$$

$$\Omega = \sin^{-1}\left[\frac{\sin 23.716}{\sin 27.755}\right];$$

$$\Omega = 59.73°.$$

$$\beta = \frac{\varphi\, avg + \Omega}{2}; \qquad (11)$$

$$\beta = \frac{23.716 + 59.73}{2};$$

$$\beta = 41.723°.$$

$$\alpha = 90 - (0,5)\cos^{-1}\left(\frac{1 - \sin \delta\, avg}{2 \sin \delta\, avg}\right) - \beta; \qquad (12)$$

$$\alpha = 90 - (0,5)\cos^{-1}\left(\frac{1 - \sin 27.755}{2 \sin \delta\, 27.755}\right) - 27.43;$$

$$\alpha = 34.580.$$

Table 10. Average Values.
Table 10. Average Values.

Parameter	Uncompacted	Compacted
φ avg, degrees	23.72	21.84
δ avg, degrees	27.76	24.49
Ω, degrees	59.73	63.80
β, degrees	41.72	42.82
α, degrees	34.58	24.64

Minimum Hopper Opening:

Using the data from Table 10 the following graphs, shown in Fig. 15 below were used to find data shown in Table 11.

Using $\alpha = 34.615$ and $\delta = 27.75$ in the graph in the figure above a value for the flow factor of 1.8 was achieved. Using the second figure on curve 3 and $\alpha = 34.615$ a value for the following was found $H(\alpha) = 1.2$.

The next step was to plot the σ_c and σ_{mc} on the Flow No-flow Criteria graph with (0,0) intercept.

The equation to the linear trend line was found to be

$$\sigma_{c1} = 1.8\, \sigma_{mc} + 4\,E{-}14 \text{ and } \sigma_{c2} = 0.677\sigma_{mc} + 75.64.$$

To obtain the critical major consolidating stress the x value for the intercept of the two flow functions is required. This is calculated below:

Trend line Equation (1): $\sigma_{c1} = 1.8\, \sigma_{mc} + 4\,E{-}14$.
Trend line Equation (2): $\sigma_{c2} = 0.677\, \sigma_{mc} + 75.64$;

Table 11. Values for compacted and uncompacted.
Таблица 11. Значения для уплотненных и неуплотненных материалов.

Parameter	Uncompacted	Compacted
δ avg, degrees	27.76	24.493
β, degrees	34.615	24.636
ff	1.8	2
H (α)	1.2	1.1

1 – Circular; 2 – Square; 3 – Roclongular (*L* > 38)
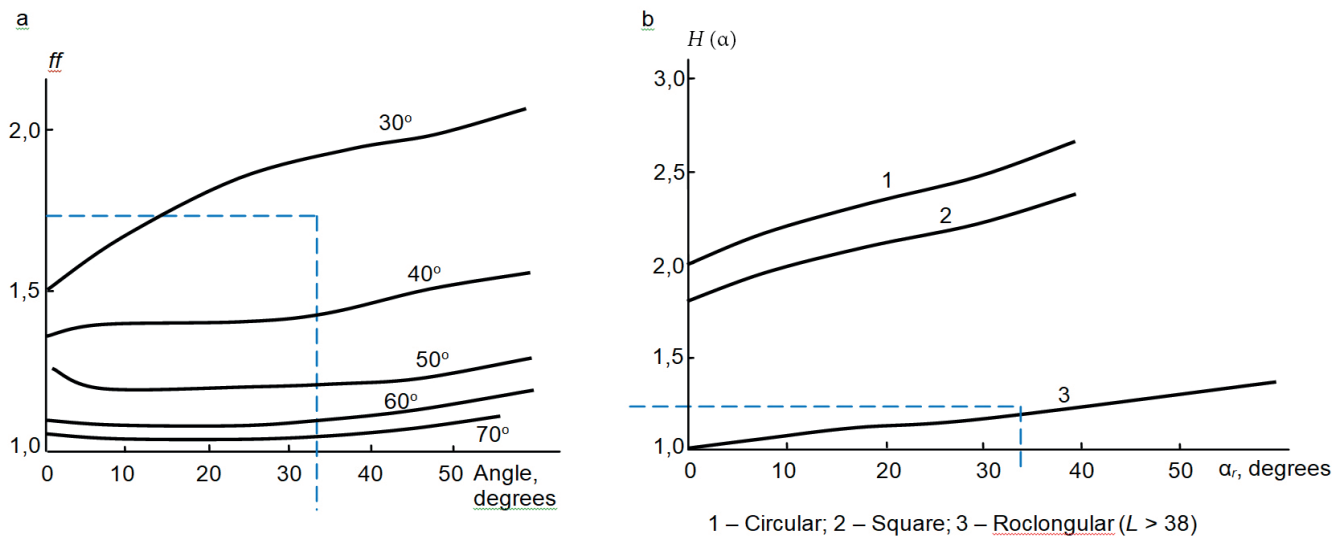
Figure 15. Empirical relation of dimensionless factor with hopper shape and half angle showing how the data in Table 10 was found [1] (a) *ff* for plane slot mass-flow silos (b) Empirical relation of dimensionless factor with hopper shape and half angle.
Рисунок 15. Эмпирическая связь безразмерного фактора с формой бункера и половинным углом, показывающая, как были найдены данные в табл. 10 [1] (a) *ff* для бункеров для хранения массовой подачи с плоской щелью (b). Эмпирическая связь безразмерного фактора с формой бункера и половинным углом.
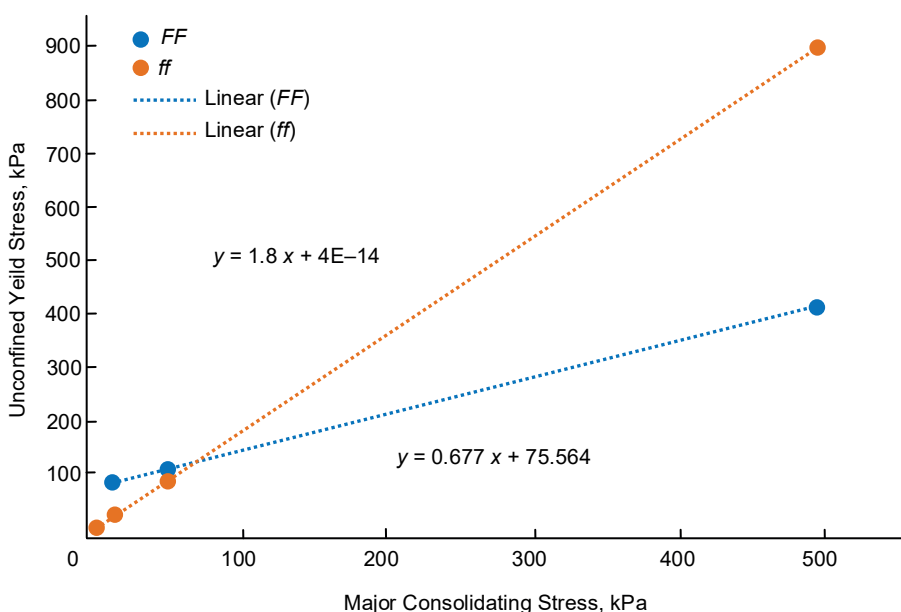
Figure 16. Flow No-flow Criteria.
Рисунок 16. Критерии отсутствия потока.

$$\sigma_{c1=}\sigma_{c2};$$

$$1.8\,\sigma_{mc} + 4\,E{-}14 = 0.677\,\sigma_{mc} + 75.64;$$

$$\sigma_{mc} = \sigma_{mc\ critical} = 67.33\ \text{kPa}.$$

The value can now be calculated as shown below:

$$\overline{\sigma} = \frac{\sigma_{mc\ critical}}{ff}; \tag{13}$$

$$\overline{\sigma} = \frac{67.33}{1.8} = 37.41\ \text{kPa};$$

From the first specific gravity experiment the specific gravity (SG) of sand was found to be 2.49. To calculate the density the following is computed whereby the density of water ($\rho\ H_2O$) is assumed to be 1000 kg/m 3 at 25 °C.

$$\rho\ \text{sand} = SG\ \text{sand} \cdot \rho\ H_2O; \tag{14}$$

$$\rho\ \text{sand} = 2.49 \cdot 1000\ \text{kg/m}^3;$$

$$\rho\ \text{sand} = 2490\ \text{kg/m}^3.$$

Now that the density of sand is known, the following equation can be used to calculate the minimum hopper opening distance.

$$B = \frac{\sigma_1 H(\alpha)}{g\rho\ \text{sand}}. \tag{15}$$

$$B = \frac{(37.41)(1.2)}{(24.90)(9.81)};$$

$$B = 0.00183\ \text{m};$$

$$B \approx 2\ \text{mm}.$$

The final results for compacted and uncompacted are shown in the following Table 12.

Table 12. Hopper half angles and openings.
Таблица 12. Половинные углы и отверстия бункера.

Parameter	Uncompacted	Compacted
α, degrees	34.615	24.636
B, mm	≈2	N/a

Note that due to having to disregard one set of the data for the compacted experiments, not enough data points were available to plot the Flow No-Flow Criteria graph and therefore it wasn't possible to calculate a minimum hopper opening width for the compacted case.

Discussion

The investigation was successful and the results from the shear cell testing allowed for a working prototype from the hopper calculations. The proposed hopper prototype work extremely well showing clear mass flow for much of the mass but steadily transformed to funnel flow once the sand level reached the angled sides. The entire lab process was a success as each group member has gained a clear understanding of the entire process; calculating the density of a bulk solid, measuring the shear force and calculating properties of a working hopper.

Referring to the results, it shows that the cohesion between uncompacted sand and acrylic is about 9 kPa with cohesion within uncompacted sand also 9 kPa, this resulted in a hopper angle of approximately 15° from the vertical. This prototype was tested purely with uncompacted sand, even though the cohesion between sand increases after compaction. The prototypes functionality with compacted sand is quite important as in many real world situations the sand will be given the chance to compact down, through transportation, weathering or extended waiting periods. In the cases stated it is important that the designed hopped work just as efficiently and should be proficiently tested in the prototype stage.

Throughout the experiment there were many errors and possible points of inaccuracy. Each stage; calculating the specific gravity (SG), preparation for experiments and running the tests all contributed to the possible error. The calculation of the SG was quite accurate as 2 separate tests were done on the same material where each result was almost identical and was very similar compared to the theoretical SG of sand. Although the preparations were carried out with great care and accuracy, it is believed that the preparation accounted for the majority of the error with in the experiment through a possible unclean shear box or Shearmatic, incorrect material measurements and discrepancies between preparation procedures. One of the tests had a difference of almost 140 g in weight to all other tests; this was likely due to a different method of filling. The applied method of preparing the shear box was to slowly fill with sand and level off using the depth gauges provided, this was an effective method/although the sand level was approximately 4 mm above the halfway when applying the sand against acrylic.

This likely meant that when applying the shear force for sand against acrylic it was not actually separating the sand from the acrylic but was separating within the sand itself.

As seen in the above table the results between the two types of tests are quite similar, although the compacted sand vs acrylic did change, likely due to when the sand was compacted it reduced the overall height of the sand closer to the centre resulting in the slipping point actually occurring between the two different materials. The Shearmatic runs a highly accurate assessment of the bulk material and is unlikely to have any errors due to mechanical faults. Although with the installation of the shear box there is a few possible weak points of examination; such as when screwing down the vertical load cell, it is apparent that the load cell applies a load to the shear box immediately as it cannot be raised enough to fully clear the top plate. Also, when entering the parameters into the Shearmatic, the top plate weight exceeds the allowable vertical weight in the system, this difference is accounted for within the calculations although the Shearmatic does not take this into consideration while applying the shear loads.

When running the uncompacted sand tests for the *SOKN* load the shear force was recorded as 73 kPa, whereas the shear force for the lOOKN load was recorded as 41 kPa and

Table 13. Hopper half angles and openings.
Таблица 13. Половинные углы и отверстия бункера.

	Uncompacted, kPa		Compacted, kPa	
Sand	Sand and Acrylic		Sand	Sand and Acrylic
9.10	9.17		4.81	5.44

the lSOKN load was 82 kPa. These results show an obvious discrepancy as in all other increasing tests they show a linear relationship. For the purposes of these sets of data the shear force of the SOKN test was altered to approximately 26 kPa, upholding the approximate linear relation.

The hopper prototype worked extremely well although the given apparatus was slightly twisted which made it extremely difficult to set a uniform opening. The varying opening slightly altered the results as one side of the hopper had a high rate mass flow whereas the opposite end had a smaller mass flow which reduced to a slight funnel flow. In general, the hopper design worked well when taking this discrepancy into consideration.

Conclusion

The mass flow acrylic bin and hopper that was requested to store bulk quantities of sand was created successfully. Creating a working prototype came from accurate flow property calculations due to the iterative shear cell and specific gravity testing. Understanding the properties of the bulk material is a vital consideration in the design process, analysing how a bulk material behaves both dry and when wetted can constitute the type of flow it will produce when exiting a hopper. The Jenike Shear Cell Test is an accurate and effective way to gather data relating to a bulk

materials behaviour when a normal and shear force is applied. The data obtained gave an accurate insight into how sand reacts under different circumstances. The data was then manipulated and plotted so stress transformations could then occur, identifying multiple key flow property constituents. Using values such as the yield loci and associative yield stresses the hopper half angle α and opening diameter B were tabulated. Approximately the optimum opening diameter B for an uncompacted system is 2mm and the hopper half angle α adjusted to 34.58°, this was tested and provided a successful mass flow hopper system. Due to having to disregard one set of the data for the compacted experiments, not enough data points were available to plot the Flow No-Flow Criteria graph and therefore it wasn't possible to calculate a minimum hopper opening width for the compacted case. Although the hopper could not be adjusted completely accurately, the result provided did give a clear indication that the iterative calculations made were correct for this particular bulk solid and hopper design. Overall the techniques used with specific gravity and shear cell testing gave a sufficient insight into the appropriate procedure for designing efficient and accurate bin and hoppers. Then substituting the values gathered into the appropriate formulae provided a successful mass flow system for the intended bulk material.

REFERENCES

1. Jager P. D., Bramante T., Luner P. E. 2015, Assessment of Pharmaceutical powder flowability using shear cell-based methods and application of Jenike's methodology. *Journal of Pharmaceutical Sciences*, vol. 104, issue 11, pp. 3804–3813. https://doi.org/10.1002/jps.24600
2. Duffy S. P., Puri V. M. 2002, Primary segregation shear cell for size-segregation analysis of binary mixtures. *KONA powder and particle journal*, vol. 20, pp. 196–207. https://doi.org/10.14356/kona.2002022 1.
3. Kyonov S., Glasser B., Muzzio F. 2015, Comparison of three rotational shear cell testers: powder flowability and bulk density. *Powder technology*, vol. 283, pp. 103–112. https://doi.org/10.1016/j.powtec.2015.04.027
4. Swize T., Osei-Yeboah F., Peterson M. L., Boulas P. 2019, Impact of shear history on powder flow characterization using a ring shear tester. *Journal of Pharmaceutical Sciences*, vol. 108, issue 1, pp. 750–754. https://doi.org/10.1016/j.xphs.2018.07.003
5. Mehos G., Eggleston M., Grenier S., Malanga C., Shrestha G., Trautman T. 2018, Designing hoppers, bins, and silos for reliable flow. *AIChE*. URL: https://www.aiche.org/resources/publications/cep/2018/april/designing-hoppers-bins-and-silos-reliable-flow
6. Dafalla M. A. 2013, Effects of Clay and Moisture Content on Direct Shear Tests for Clay-Sand Mixtures. *Advances in Materials Science and Engineering*, vol. 4, pp. 1–8. https://doi.org/10.1155/2013/562726
7. Lee Y. J., Yoon W. B. 2015, Flow behaviour and hopper design for black soybean powders by particle size. *Journal of Food Engineering*, vol. 144, pp. 10–19. https://doi.org/10.1016/j.jfoodeng.2014.07.005
8. Søgaard S. V., Olesen N. E., Hirschberg C., Madsen M. H., Allesø M., Garnaes J., Rantanen J. 2017, An experimental evaluation of powder flow predictions in small-scale process equipment based on Jenike's hopper design methodology. *Powder technology*, vol. 321, pp. 523–532. https://doi.org/10.1016/j.powtec.2017.08.006
9. Ketterhagen W. R., Curtis J. S., Wassgren C. R., Hancock B. C. 2009, Predicting the flow mode from hoppers using the discrete element method. *Powder Technology*, vol. 195, issue 1, pp. 1–10. https://doi.org/10.1016/j.powtec.2009.05.002
10. Wang Y., Koynov S., Glasser B. J., Muzzio F. J. A method to analyse shear cell data of powders measured under different initial consolidation stresses. *Powder Technology*, vol. 294, pp. 105–112. https://doi.org/10.1016/j.powtec.2016.02.027
11. Barletta D., Berry R. J., Larsson S. H., Lestander T. A., Poletto M., Ramírez-Gómez A. 2015, Assessment on bulk soilds best practice techniques for flow characterization and storage/handling equipment design for biomass materials of different classes. *Fuel Processing Technology*, vol. 138, pp. 540–554. https://doi.org/10.1016/j.fuproc.2015.06.034
12. Junfu J., Fitzpatrick J., Cronin K., Fenelon M. A., Miao S. 2017, The effects of fluidised bed and high shear mixer granulation processes on water adsorption and flow properties of milk protein isolate powder. *Journal of Food Engineering*, vol. 192, pp. 19–27. https://doi.org/10.1016/j.jfoodeng.2016.07.018
13. Fernandez J. W., Cleary P. W., McBride W. 2011, Effect of screw design on hopper drawdown of spherical particles in a horizontal screw feeder. *Chemical Engineering Sciences*, vol. 66, issue 22, pp. 5585–5601. https://doi.org/10.1016/j.ces.2011.07.043
14. Wang Y., Snee R. D., Meng W., Muzzio F. J. 2016, Predicting flow behaviour of pharmaceutical blends using shear cell methodology: A quality by design approach. *Powder Technology*, vol. 294, pp. 22–29. https://doi.org/10.1016/j.powtec.2016.01.019
15. Michael J.Carr, Alan W.Roberts, Craig A.Wheeler, A revised methodology for the determination of bulk material cohesion and adhesion, Advanced Powder Technology, Volume 30, Issue 10, October 2019, Pages 2110-2116

Испытание на сдвиг и конструкция бункера

Лукас АРНОЛЬД[1*]
Тарун КУМАР[1**]
Джошуа КОУЛИ[1***]
Грег УИТЛИ[1****]
Рендаге Сачини Сандипа ЧАНДРАСИРИ [2*****]

[1]Университет Джеймса Кука, Таунсвилл, Австралия
[2]Университет Коломбо, Шри-Ланка

Аннотация

Актуальность работы. Конструкция резервуара и бункера является наиболее часто используемым техническим средством хранения материалов, поскольку это система с подачей самотеком и обычно используется для хранения материалов, таких как сельскохозяйственное зерно, а также добытых полезных ископаемых, таких как песок и уголь. Массовый поток, который является наиболее желательным типом подачи, предполагает, что сыпучий материал перемещается равномерно со всеми частицами в движении, пока весь материал не выйдет из бункера. Другие типы потока с бункерами с плоским дном и неглубокими бункерами не считаются идеальными, поскольку при этой конструкции возникают такие проблемы, как выгибание и образование дырок. Проблема с такой конструкцией заключается в том, что часть материала застаивается в бункере, это может быть дорогостоящим, так как если сыпучий материал застревает, со временем может происходить разрушение. Это можно наблюдать для воронкообразного и расширяющегося потока, когда «крысиные норы» и выгибания возникают из-за застойного материала.

Цель исследования заключается в разработке нового акрилового бункера и резервуара массовой подачи для хранения большого количества песка без застоя или разрушения.

Методология. Были проведены две отдельные экспериментальные процедуры, включая измерение удельного веса песка, испытание на сдвиг, и разработана окончательная конструкция бункера. Затем данные обрабатывались и наносились на график преобразования напряжений и определялись несколько ключевых составляющих свойств потока. С использованием таких значений, как места текучести и ассоциативные напряжения текучести, были сведены в таблицу половинный угол бункера α и диаметр отверстия *B*.

Результаты и выводы. Оптимальный диаметр отверстия *B* для неуплотненной системы составляет 2 мм, а половинный угол бункера α отрегулирован до 34,58°. Это было проверено и обеспечило успешное тестирование системы бункера массовой подачи. В целом методы, использованные для испытаний на удельную массу и сдвиговую ячейку, дали достаточное представление о соответствующей процедуре проектирования эффективных и точных резервуаров и бункеров. Затем подстановка собранных значений в соответствующие формулы обеспечила успешное тестирование системы массовой подачи предполагаемого сыпучего материала, которым является песок.

Ключевые слова: бункер, свойства текучести, минералы, свойства сыпучего материала, геометрическая форма.

ЛИТЕРАТУРА

1. Ягер П. Д., Браманте Т., Лунер П. Э. Оценка текучести фармацевтического порошка с использованием методов на основе сдвиговых ячеек и применения методологии Джденике // Журнал фармацевтических наук. 2015. Т. 104, вып. 11. С. 3804–3813. https://doi.org/10.1002/jps.24600
2. Даффи С. П., Пури В. М. Сдвиговая ячейка для первичной сегрегации для анализа разделения бинарных смесей по размеру // Журнал о порошках и частицах KONA. 2002. Т. 20. С. 196–207. https://doi.org/10.14356/kona.2002022
3. Кёнов С., Глассер Б., Муццио Ф. Сравнение трех тестеров ротационных камер сдвига: сыпучесть порошка и насыпная плотность // Порошковая технология. 2015. Т. 283. С. 103–112. https://doi.org/10.1016/j.powtec.2015.04.027
4. Свиз Т., Осей-Йебоа Ф., Петерсон М. Л., Булас П. Влияние истории сдвига на характеристики потока порошка с помощью кольцевого измерителя сдвига // Журнал фармацевтических наук. 2019. Т. 108, вып. 1. С. 750–754. https://doi.org/10.1016/j.xphs.2018.07.003
5. Мехос Г., Эгглстон М., Гренье С., Маланга К., Шреста Г., Траутман Т. Проектирование бункеров и резервуаров для обеспечения надежного потока // AIChE. 2018. URL: https://www.aiche.org/resources/publications/cep/2018/april/designing-hoppers-bins-and-silos-reliable-flow

✉Lukas.arnold@my.jcu.edu.au
**Tarun.kumar@my.jcu.edu.au
***Joshua.cowley@my.jcu.edu.au
****greg.wheatley@jcu.edu.au
https://orcid.org/0000-0001-9416-3908
*****sachini.chandrasiri7@gmail.com
https://orcid.org/0000-0003-4713-9088

6. Дафалла М. А. Влияние содержания глины и влаги на испытания на прямой сдвиг для смесей глины и песка // Достижения в области материаловедения и инженерии. 2013. Т. 4. С. 1–8. https://doi.org/10.1155/2013/562726

7. Ли Ю. Дж., Юн В. Б. Характеристики потока и конструкция бункера для порошков черной сои по размеру частиц // Журнал пищевой инженерии. 2015. Т. 144. С. 10–19. https://doi.org/10.1016/j.jfoodeng.2014.07.005

8. Согаард С. В., Олесен Н. Э., Хиршберг К., Мадсен М. Х., Аллесо М., Гарнаес Дж., Рантанен Дж. Экспериментальная оценка прогнозирования потока порошка в маломасштабном технологическом оборудовании на основе методологии проектирования бункера Дженике // Порошковая технология. 2017. Т. 321. С. 523–532. https://doi.org/10.1016/j.powtec.2017.08.006

9. Кеттерхаген В. Р., Кертис Дж. С., Вассгрен К. Р., Хэнкок Б. С. Прогнозирование режима потока из бункеров с использованием метода дискретных элементов // Порошковая технология. 2009. Т. 195, вып. 1. С. 1–10. https://doi.org/10.1016/j.powtec.2009.05.002

10. Ван Ю., Койнов С., Глассер Б. Дж., Муццио Ф. Дж. Метод анализа данных ячеек сдвига порошков, измеренных при различных начальных напряжениях консолидации // Порошковая технология. 2016. Т. 294. С. 105–112. https://doi.org/10.1016/j.powtec.2016.02.027

11. Барлетта Д., Берри Р. Дж., Ларссон С. Х., Лестандер Т. А., Полетто М., Рамирес-Гомес А. Оценка передовых методов работы с сыпучими грунтами для определения характеристик потока и проектирования оборудования для хранения/обработки материалов из биомассы различных классов // Технология переработки топлива. 2015. Т. 138. С. 540–554. https://doi.org/10.1016/j.fuproc.2015.06.034

12. Джунфу Дж., Фитцпатрик Дж., Кронин К., Фенелон М. А., Миао С. Влияние процессов грануляции в псевдоожиженном слое и смесителя с большим усилием сдвига на адсорбцию воды и реологические свойства порошкового изолята молочного белка // Журнал пищевой инженерии. 2017. Т. 192. С. 19–27. https://doi.org/10.1016/j.jfoodeng.2016.07.018

13. Фернандес Дж. У., Клири П. У., Макбрайд У. Влияние конструкции шнека на усадку бункера сферических частиц в горизонтальном шнековом питателе // Химико-инженерные науки. 2011. Т. 66, вып. 22. С. 5585–5601. https://doi.org/10.1016/j.ces.2011.07.043

14. Ван Й., Сни Р. Д., Мэн В., Муццио Ф. Дж. Прогнозирование поведения потока фармацевтических смесей с использованием методологии сдвиговых ячеек: подход к качеству, не уступая дизайну // Порошковая технология. 2016. Т. 294. С. 22–29. https://doi.org/10.1016/j.powtec.2016.01.019